Anti-Stokes luminescence in bismuth-doped high-germania core fibres

S.V. Firstov, E.G. Firstova, A.V. Kharakhordin, K.E. Riumkin, S.V. Alyshev, M.A. Melkumov, E.M. Dianov

Abstract. **This paper presents a study of anti-Stokes luminescence in optical fibres with a bismuth-doped $\sim 50\%\mathrm{GeO_2}-50\%\mathrm{SiO_2}$ glass core under IR excitation. The anti-Stokes luminescence intensity has been measured as a function of temperature in the range 77–300 K. From these data, we have evaluated the activation energy for the thermal quenching of anti-Stokes luminescence in the visible and IR spectral regions. A mechanism of anti-Stokes luminescence in this type of optical fibre has been proposed.**

Keywords: bismuth-doped optical fibre, anti-Stokes luminescence.

1. Introduction

Bismuth-doped optical fibres have unique luminescence properties, which have made it possible to create a family of fibre lasers and optical amplifiers operating in various parts of the near-IR spectral region [1–3]. The last wavelength range that has been covered by bismuth-doped fibre lasers to date is 1600–1800 nm. This was achieved owing to the advent of bismuth-doped high-germania glass core fibres, which were found to have an optical gain band peaking near 1730 nm. At the same time, despite the significant advances in designing optical devices based on such fibres, they remain poorly studied gain media, which makes it impossible to fully assess their potentialities.

In this paper, major attention is paid to anti-Stokes luminescence in this type of optical fibre. This issue has been addressed in a number of studies [4–6], in which IR excitation was shown to produce visible luminescence bands. Anti-Stokes luminescence in such fibre was studied in detail under sequential excitation with two IR photons. This made it possible to demonstrate that the anti-Stokes luminescence was due to bismuth-related active centres (BACs) and identify the main transitions responsible for it. It is worth noting that the anti-Stokes luminescence intensity was shown to be considerably higher at low temperatures, but the temperature behaviour of anti-Stokes luminescence has not yet been systematically studied.

In this paper, we report a detailed study of the effect of bismuth concentration and active fibre temperature on anti-

S.V. Firstov, E.G. Firstova, A.V. Kharakhordin, K.E. Riumkin, S.V. Alyshev, M.A. Melkumov, E.M. Dianov Fiber Optics Research Center, Russian Academy of Sciences, ul. Vavilova 38, 119333 Moscow, Russia; e-mail: fir@fo.gpi.ru

Stokes luminescence. Such studies are expected to extend our fundamental understanding of processes occurring in such materials, which is important in producing efficient laser media.

2. Experimental

For our experiments, we produced a series of preforms by MCVD. Their core consisted of $\sim 50\%\mathrm{GeO_2}-50\%\mathrm{SiO_2}$ glass containing different bismuth concentrations, no higher than ~ 0.1 wt%. The second mode cutoff wavelength was about 1.2 μm and the core diameter was near 2.5 μm. Anti-Stokes luminescence spectra were measured as schematised in Fig. 1.
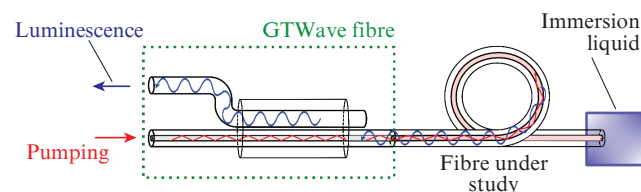

Figure 1. Schematic of luminescence measurements with the use of GTWave fibre.

We used a GTWave fibre design containing two fibres: one fibre had a core and was used to launch pump light into an active fibre, and the other fibre was used to detect luminescence. Pump light was coupled into the core of the active fibre and the luminescence to be detected propagated through its cladding, partially penetrating the coreless fibre. The active fibre was stripped of its protective polymer coating, which was nonreflective in the case of fibres intended for core pumping. This allowed the luminescence signal to propagate through the cladding with no significant loss. To reduce reflection of the pump light from the output end face of the active fibre, it was placed in an immersion liquid. Excitation was provided by a supercontinuum source (Fianium SC450) fitted with an AODS 20160-8 acousto-optic filter (Crystal Technology Inc.) for cutting a spectral band of width $\Delta\lambda \sim 5$ nm from the broad supercontinuum spectrum. In this study, we used light in the range 850–1000 nm because excitation at these wavelengths ensures the highest anti-Stokes luminescence intensity. Luminescence was detected in the range 400–800 nm using an Ocean Optics QE65000 spectrometer. In data processing, the luminescence spectra were normalised to the transmission function of the GTWave fibre channels, the excitation power and the spectral sensitivity of the spectrometer.

A similar configuration was used in our low- and high-temperature measurements. In the low-temperature experiments, the fibre was placed in a thermostat, which maintained a temperature from ~ 70 to 300 K with an accuracy of 5 K. In the high-temperature measurements (up to 600 K), the active fibre was heated by a Nakal tube furnace having an about 40-cm-long isothermal zone.

3. Results and discussion

Figure 2a presents a typical anti-Stokes luminescence spectrum under excitation at a wavelength of 925 nm. The spectrum shows two, rather narrow bands, peaking at 485 and 660 nm. The inset in Fig. 2a shows measured luminescence excitation spectra for both bands. Anti-Stokes luminescence in similar samples was the subject of previous work [5], where the main optical transitions responsible for the observed
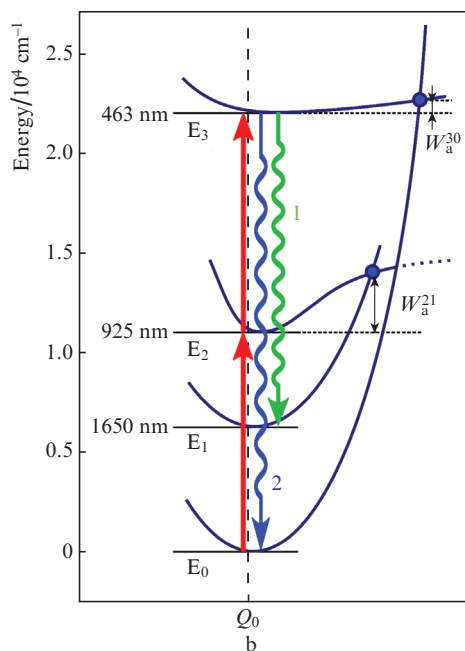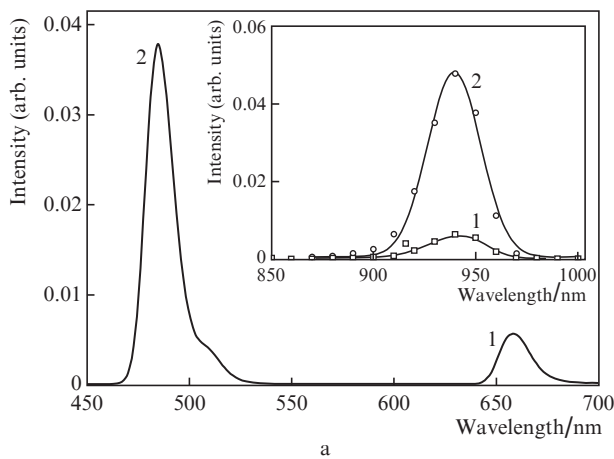
bands were identified. The present results demonstrate that both luminescence bands arise from the same BAC, as evidenced by the good agreement between the positions and shapes of their excitation bands.

The radiative transitions of the BACs, responsible for the anti-Stokes luminescence from the higher energy level E_3, and the optical transitions of the BACs upon pump absorption at a wavelength of 925 nm are represented in the energy level diagram of the BACs in Fig. 2b [7], which was constructed using the present results and previously reported data [6]. The diagram suggests that there are at least two possible mechanisms of anti-Stokes luminescence from the E_3 level: (1) as a result of a sequential absorption of two pump photons, accompanied by a transition of the BAC from the ground state E_0 to the excited level E_3 through the intermediate level E_2 (excited state absorption, ESA), and (2) as a result of nonradiative excitation energy transfer between neighbouring BACs (energy transfer upconversion, ETU) in an excited state (E_2 level), a process in which one of the active centres passes to higher level, and the other, to the ground state.

To find out, which of the excitation mechanisms was operative, we measured the ratio of the anti-Stokes luminescence intensities ($E_3 \rightarrow E_1$ and $E_3 \rightarrow E_0$ transitions) to the Stokes luminescence intensity ($E_2 \rightarrow E_0$) at different pump powers. The results are presented in Fig. 3. It is seen that this ratio remains constant over the entire range of pump powers studied. These results provide additional evidence that both anti-Stokes luminescence bands are due to transitions from the same energy level. It follows from analysis of the present data that the population of the third excited level, N_3, is a linear function of the population of the second excited level, N_2. Thus, the population of the third energy level is directly proportional to the pump power: $N_3 \backsim N_2 \backsim P$ and hence $I_{AS} \backsim I_S \backsim P$ (here, I_{AS} and I_S are the anti-Stokes and Stokes luminescence intensities). This situation differs from the behaviour of anti-Stokes luminescence in standard cases of ETU and ESA [8]:

$$I_S \backsim P, \quad I_{AS} \backsim P^2, \text{ weak ETU,}$$

$$I_S \backsim P^{1/2}, \quad I_{AS} \backsim P, \text{ strong ETU,}$$

$$I_S \backsim P, I_{AS} \backsim P^2, \text{ weak ESA,} \tag{1}$$

Figure 2. (a) Anti-Stokes luminescence spectrum under excitation at a wavelength of 925 nm (inset: luminescence excitation spectra of bands 1 and 2); (b) energy level diagram of the BACs, showing the radiative transitions (1 and 2) responsible for the corresponding characteristic luminescence bands.
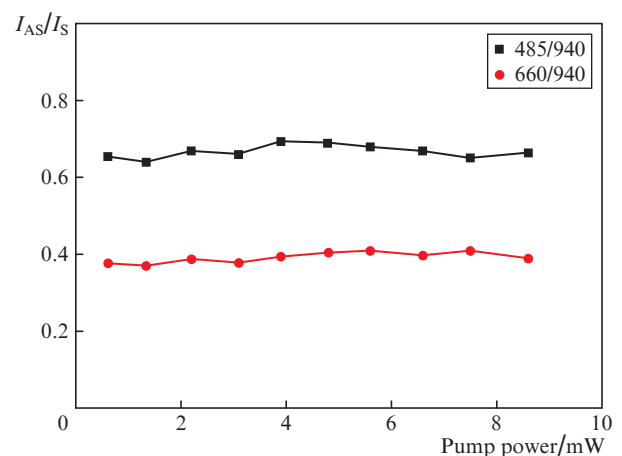

Figure 3. Ratios of the anti-Stokes luminescence intensities I_{AS} at $\lambda = 660$ and 485 nm to the Stokes luminescence intensity I_S at $\lambda = 940$ nm as functions of the pump power at $\lambda = 925$ nm.

$I_S \approx$ const, $\quad I_{AS} \, \infty \, P$, strong ESA.

At the same time, it is seen in the energy level diagram of the BACs in Fig. 2b that the $E_3 \rightarrow E_2$ transition is identical in energy to the $E_2 \rightarrow E_0$ transition. Therefore, the Stokes luminescence intensity at a wavelength near 940 nm depends on not only the population of the E_2 level but also that of the E_3 level. As a result, the anti-Stokes and Stokes luminescence intensities can vary linearly with pump power. As follows from the above relations (1), this situation occurs only in the case of a strong pump absorption by active centres in an excited state. Thus, we are led to conclude that the most likely mechanism of the anti-Stokes luminescence is a sequential absorption of two photons (ESA) rather than excitation energy transfer between active centres.

As pointed out repeatedly (see e.g. Ref. [3]), the absorption band located near 1650 nm is attributable to the BACs because its intensity is a linear function of total bismuth concentration in the fibre core. In addition, this spectral range includes a nonsaturable absorption, which is presumably due to bismuth clusters, as evidenced by the nonlinear dependence of this absorption on bismuth concentration. Bismuth clustering occurs in bismuth-doped fibres based on P_2O_5- and/or Al_2O_3-doped silica glass. As shown recently [9], bright anti-Stokes luminescence in bismuth-rich aluminosilicate fibres is due to this type of centre.

In view of this, it was reasonable to carry out such a study of anti-Stokes luminescence in bismuth-doped high-germania fibres. We measured the 485-nm luminescence intensity under 925-nm excitation for fibres with different absorption coefficients at $\lambda = 1650$ nm. For a further comparative analysis of the data obtained, the luminescence was measured at certain lengths of the active fibre, which depended on active absorption. The fibre length was varied from 5 to 50 cm.

The measurement results are presented in Fig. 4. It is seen that, with increasing bismuth concentration, the anti-Stokes luminescence intensity rises at active absorption levels below about 2 dB m^{-1}. The reason for this is that, at such bismuth concentrations, the fibres contain predominantly BACs. Further raising the total bismuth concentration leads to luminescence quenching, which is probably due to the formation of bismuth clusters. This is supported by the data in Fig. 4, which shows the measured nonsaturable loss as a function of active absorption. Thus, it can be stated with certainty that
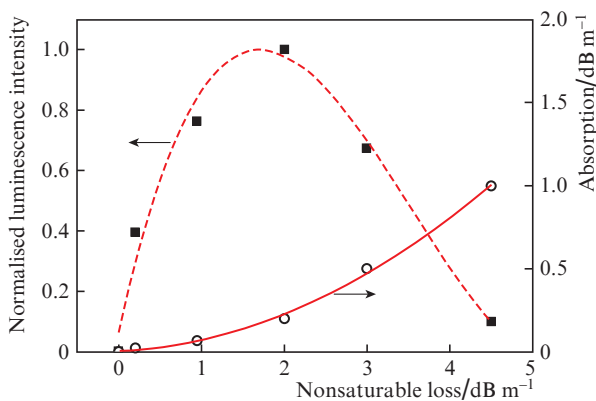
the anti-Stokes luminescence is due to bismuth-related active centres which differ in structure from bismuth dimers and other bismuth clusters that can coexist with BACs in a glass host.

The anti-Stokes luminescence intensity was measured as a function of temperature in the range $\sim 77-300$ K. Figure 5 shows anti-Stokes luminescence spectra (the band peaking at a wavelength of 485 nm) at different bismuth fibre temperatures. With increasing temperature, the luminescence intensity decreases monotonically, whereas the spectral position and width of the luminescence band remain unchanged. This points to thermal quenching of luminescence. The dependence of the 485-nm anti-Stokes luminescence intensity on fibre temperature is shown in Fig. 6a in greater detail. It is seen that, at temperatures above 250 K, the luminescence intensity is determined by the sensitivity limit of the measuring system.
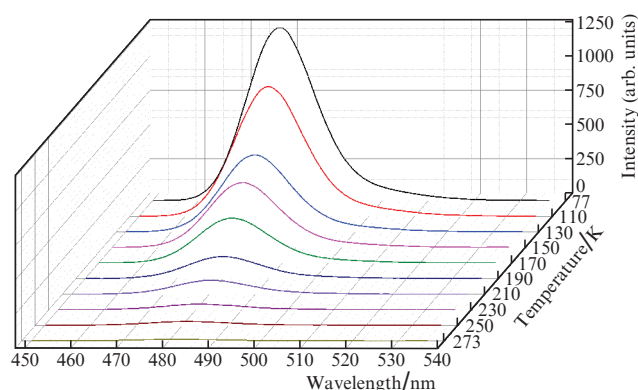

Figure 5. Anti-Stokes luminescence intensity as a function of wavelength and temperature under 925-nm excitation at a pump power of ~ 1 mW.

We assume that, in this case, we observe thermal quenching of luminescence by the Mott–Seitz mechanism [7], according to which adiabatic potential curves corresponding to different electronic states of an active centre have intersection points. This makes a transition between electronic states possible if the thermal energy is sufficient for surmounting a potential barrier referred to as the activation energy for luminescence quenching. The temperature dependence of luminescence intensity, $I(T)$ can then be represented by the formula

$$I(T) = \frac{I_0}{1 + C\exp(-W_a/kT)}, \qquad (2)$$

where I_0 is the initial anti-Stokes luminescence intensity (at 77 K in our case); C is a dimensionless constant; W_a is the activation energy for the thermal quenching of luminescence (Fig. 2b); and k is the Boltzmann constant.

It is seen from Fig. 6a that formula (2) adequately describes the measured anti-Stokes luminescence intensity as a function of temperature for the bismuth-doped fibres. This allowed us to determine the activation energy W_a^{30} (Fig. 2b), which was found to be 70 meV. In addition, relation (2) allows us to describe the thermal quenching of luminescence from the E_2 level, accompanied by a concurrent increase in the intensity of luminescence from the E_1 level (Fig. 6b). The activation energy W_a^{21} is in this case considerably higher (Fig. 2b): about 390 meV.

Figure 4. Normalised intensity of the anti-Stokes luminescence with a peak emission wavelength of 485 nm and nonsaturable loss coefficient as functions of active absorption at $\lambda = 1650$ nm.

$$I/I_0 = \{1 + 500\exp[-(70 \text{ meV})/kT]\}^{-1}$$

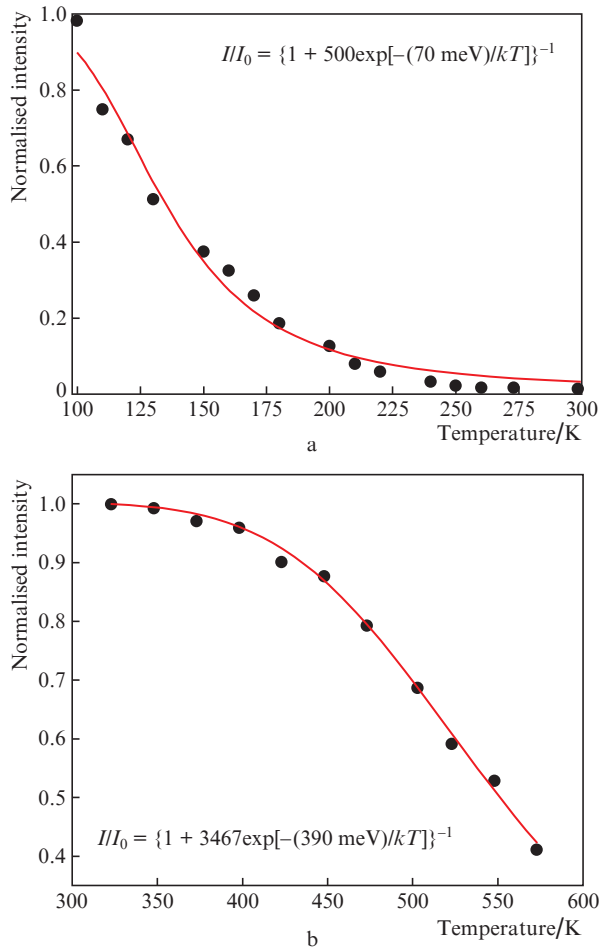$$I/I_0 = \{1 + 3467\exp[-(390 \text{ meV})/kT]\}^{-1}$$

Figure 6. (a) 485-nm anti-Stokes luminescence intensity and (b) 940-nm Stokes luminescence intensity as functions of temperature for the bismuth-doped fibre. The activation energies extracted from these data (70 and 390 meV) were used to more accurately determine the energy level diagram of the bismuth-related active centres in Fig. 2b.

4. Conclusions

We have presented results of measurements of anti-Stokes luminescence parameters in optical fibres having an $\sim 50\% \text{ GeO}_2 - 50\% \text{ SiO}_2$ glass core doped with less than 0.1 wt% bismuth. The ratio of the intensities of anti-Stokes and Stokes luminescence bands has been determined as a function of pump power at a wavelength of 925 nm. Analysis of these data has led us to assume that the anti-Stokes luminescence is due to sequential absorption of two excitation photons. The anti-Stokes luminescence intensity has been determined as a function of the active absorption coefficient near a wavelength of 1650 nm. These data also suggest that the observed anti-Stokes luminescence bands are due to BACs. The intensity of the shorter wavelength anti-Stokes luminescence band (peaking at a wavelength of 485 nm) and that of the 940-nm Stokes luminescence have been measured as functions of temperature in the ranges 77–300 and 300–575 K, respectively. The results demonstrate that the spectral position and shape of the anti-Stokes luminescence band vary little with temperature, whereas its intensity decreases monotonically with increasing temperature. Our data have been used to evaluate the activation energy for the thermal quenching of luminescence at wavelengths of 485 and 940 nm. The results have allowed

us to more accurately determine the mutual position of the energy levels of the bismuth-related active centres.

References

1. Dianov E.M. *Light: Sci. Appl.*, **1**, e1 (2012).
2. Bufetov I.A. et al. *IEEE J. Sel. Top. Quantum Electron.*, **20**, 0903815 (2014).
3. Firstov S.V. et al. *IEEE J. Sel. Top. Quantum Electron.*, **24**, 0902415 (2018).
4. Xie W., Qiu Y., Wang Y. *Laser Phys.*, **23**, 015702 (2012).
5. Firstov S.V. et al. *Opt. Express*, **21**, 18408 (2013).
6. Firstov S.V. et al. *Opt. Express*, **19**, 19551 (2011).
7. Chen R., Pagonis V. *Thermally and Optically Stimulated Luminescence: a Simulation Approach* (New Jersey: John Wiley & Sons, 2011) p. 22.
8. Pollnau M., Gamelin D.R., Luthi S.R., Gudel H.U., Hehlen M.P. *Phys. Rev. B*, **61**, 3337 (2000).
9. Firstov S.V. et al. *Quantum Electron.*, **46**, 612 (2016) [*Kvantovaya Elektron.*, **46**, 612 (2016)].